Penerbit Akademia Baru

Journal of Advanced Research in Fluid Mechanics and Thermal Sciences

Journal homepage: www.akademiabaru.com/arfmts.html
ISSN: 2289-7879

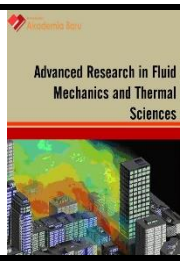


# Natural Convection Heat transfer in a Concentric Annulus Vertical Cylinders embedded with Porous Media

Open Access

Mohammed Ali Mahmood[1], Mustafa Abdulsalam Mustafa[1], Mohammad M. Al-Azzawi[1], Atheer Raheem Abdullah[1,*]

[1] Refrigeration and Air Conditioning Engineering Department, Faculty of Engineering, Al-Rafidain University Collage, Baghdad, Iraq

**ARTICLE INFO**

***Article history:***
Received 11 October 2019
Received in revised form 11 November 2019
Accepted 15 November 2019
Available online 4 March 2020

***Keywords:***
Natural Convection; Porous Media; Concentric Annulus; Finite Volume Method

**ABSTRACT**

The prediction of heat transfer due to natural convection in vertical enclosures of concentric cylindrical annular form has received considerable attention because of numerous heat transfer applications. A Numerical investigation of the natural convection heat transfer between two isothermal concentric vertical cylinders inserted with porous medium was studied. The numerical solutions were obtained for a Rayleigh number (Ra) ranging between (300-400) and Prandtl number=0.7. Finite volume technique with the SIMPLE algorithm was used to solve the Navier–Stokes and energy equations using Fluent v.15.0 software. One type of boundary conditions has been considered for the inner cylinder, where its wall was heated by applying a uniform heat flux with different ranges (300-450W/m$^2$). The predicted results were presented in terms of temperature profiles and stream functions for different ratio (r/R) and Ra to show the behavior of the temperature fields and fluid flow. The simulated data of the average Nusselt number values have been compared under the same boundary conditions to similar results of previous works and good agreement was obtained. The predicted results revealed that the average Nusselt number was a function of varied Rayleigh number and non-dimensional parameter of (r/R). Results also showed an increase in the natural convection as heat flux increases leads to an improve in the heat transfer process and the average Nusselt number increases with Ra and (r/R) ratio increases.



## 1. Introduction

In recent years, natural convection heat transfer in a cylindrical annulus has attracted much attention with relation to thermal storage systems, solar collectors, spent nuclear air fuel cooling, nuclear reactors, aircraft fuselages insulation, cooling of electrical equipments. The vertical convection isothermal cylinders were used pressurized gas underground electric transition cables; therefore, many large-scale experiments have been performed to study the interaction between

* *Corresponding author.*
*E-mail address: atheerraheem@yahoo.com (Atheer Raheem Abdullah)*

hydrodynamic and thermal influences in such geometries. A comprehensive work on heat transfer by natural convection in concentric annuli may be found in [1]. In this paper, we present a brief review of selected experimental papers and related theoretical studies.

Projahn and Beer [2] was investigated the effect of modified Prandtl numbers on the laminar convective heat transfer in a vertical two concentric and eccentric cylinders numerically. Numerical transformation method was employed for mapping the complex physical domains to overcome the difficulties associated with this region on a rectangle. During the simulation, in spite of two separating computer programs depending on variant formulations of the partial governing equations were employed, but close results were obtained. The relation between local heat transfer coefficient and various Rayleigh numbers are presented for the first time. The simulated data revealed that the rates of local heat transfer are depending on the Rayleigh number and as well as the Prandtl number.

El-Shaarawi *et al.,* [3] carried out a numerical study to investigate the transient conjugated heat transfer phenomena under thermally and hydrodynamically fully developed flow in a concentric annulus. The governing equation were solved using a finite-difference scheme to find the flow characteristics. The flow under laminar condition and constant physical properties were considered. The external tube outer surface is maintained adiabatic while the inside tube wall is subjected to isothermal temperature that was changed by a step to initiate the thermal transient. The influence of the diffusivity ratio and fluid-solid conductivity ratio on the thermal flow behavior have been studied. The simulated results are obtained for fluid flow of Pr = 0.7 and different wall thicknesses. The results show that the walls thicknesses have a significant influence on the transient conjugated heat transfer.

Maged and Negm [4] presented numerical investigation to study the laminar conjugate natural convection heat transfer phenomena in vertical concentric annuli with open-ended. A technique of finite difference method was employed to solve the Navier-Stokes and energy equations. The inner tube wall is insulated while the outer tube surface is heated isothermally. The working Newtonian fluid is air of Pr. =0.7 with ratio of radius (r/R =0.5). The influence of ratio of fluid-solid thermal conductivity (KR) has been studied, and significant effects were found on the parameters of steady heat transfer.

Teertstra and Yovanovich [5] presented a theoretical and experimental model for heat transfer in in a horizontal circular annulus filling with a porous medium by free convection and under constant heat flux condition. They carried out a comparison between the experimental data and the models with focusing on some recommendations. The aim of this study is to find out the effect of diameter ratio and isothermal condition on coefficient of heat transfer with the presence of porous medium and Rayleigh number, then find a relationship between Nusselt number with diameter ratio for various Rayleigh number and the relationship between Nusselt number and Rayleigh number with different diameter ratios.

Akeel [6] carried out experimental study to find the natural convective heat transfer characteristics in a vertical concentric cylindrical annulus. The inner surface of cylinder is subjected to constant heat flux ranging from 58.2 W/m$^2$ to 274.31 W/m$^2$, while the outer cylinder surface is kept at ambient temperature. The annulus has a length of 1.2m with a radius ratio of 0.555. The experimental results showed that the increases in heat flux leads to an enhance in the process of heat transfer resulting from an increasing in the natural convection. An empirical correlation for average Nusselt number was concluded as a function of Rayleigh number. It was also concluded that the buoyancy influence is little at the entrance region of annulus, but at the downstream region it was increased.

Ayad and Jasim [7] studied numerically the problem of transient natural convection heat transfer in isothermally heated horizontal cylindrical annuli. The inner wall is heated while the outer wall is

kept cool. During the laminar condition, the Grashof number modified from $1x10^2$ to $1x10^5$ in Air. Both of equation of stream function and alternating direction implicit (ADI) method were used to solve the vorticity and energy equations. The Nusselt number, velocity vector and temperature distribution were obtained during the simulation as well as the influence of diameter ratio on these parameters. The change of Grashof number and Prandtl number were studied simultaneously. The simulated data are summarized by Grashof number versus average Nusselt number curves with Prandtl number as a parameter which indicate the convection heat transfer obtained from the cylinders. Also, good agreement is obtained as compared to the published previous data.

Nicholas *et al.,* [8] demonstrated numerical study natural convection heat transfer and fluid flow to validate the simulation code with respect to the experimental results in an annulus of horizontal concentric cylinders. The equivalent thermal conductivity correlation for small radii was applied in this investigation and found it was suitable for larger radii up to a Rayleigh number of less than $10^8$ for both laminar and turbulent flow regimes, but for a wide range of Rayleigh numbers ($Ra > 10^8$) in the turbulent region the empirical correlation over predict rates of heat transfer. The comparison between experimental and CFD results for temperature data and local coefficient of heat transfer indicates that the simulations sufficiently represent the physics of flow in the annulus, but at transition to turbulence region a model of turbulence flow is necessary to handle transitional influences.

Hiroki *et al.,* [9] studied experimentally the heat transfer between two coaxial cylinders under constant heat flux condition. Low -pressure method was used to measure the coefficient of thermal accommodation and the coaxial cylinders' geometry has been experimentally implemented. Large radius ratio of cylinders and high temperature difference with a wide range of high pressure were applied during the experimental setup. The nonlinear S-model kinetic equation was used to simulate the heat flux in order to verify assumptions in the extraction of accommodation coefficient. Very good compatibility was obtained between the simulated and the measured heat flux. It was also observed that the coefficient of the thermal accommodation depends on the temperature. The uncertainties analyses for the measurements were proposed besides to the errors resulting from the procedure of accommodation coefficient extraction.

Xing Yuan *et al.,* [10] presented study to simulate the natural convection in horizontal concentric annuli of various modified shapes. The outer and inner walls are remained at a constant temperature. Four shapes were of different inner entity, such as cylindrical, square, elliptical, or triangular. Isotherms contours and streamlines figures are exhibited to represent the thermal fields and flow. Predicted correlations were developed to find the overall heat transfer associated with radiation based on average Nusselt number. The results revealed that the corners presence and more big top space improves the rate of heat transfer. Besides, the radiation form surface plays significant role in the increasing of the performance of the overall heat transfer.

Ebrahim *et al.,* [11] carried out numerical simulation to investigate the free convection heat transfer in horizontal annuli using $Al_2O_3$ nanofluids. The two-dimensional governing equations of continuity, momentum and energy are solved numerically using Fluent code. Three different volume of fraction 1%, 2%, and 5% are used at a various Rayleigh numbers $10^3$, $10^4$, and $10^5$. The simulated data demonstrated that the using of nanoparticles and increasing of its concentrations leads to enhance the rate of heat transfer. The maximum improvement of the average Nusselt number is about 30% at $Ra = 10^3$, while the minimum augmentation is 14% at $Ra = 10^5$. It was observed also that the increasing of Rayleigh number leads to increase the average Nusselt number for all studied cases and the volume of fraction 5% at $Ra = 10^3$ gives greater improvement in the heat transfer to the cold tube by about 23% as compared to the pure water. The solution is verified by comparing the data with previously published work, and good agreement is obtained.

Xiufeng and Song [12] investigated numerically the natural convection heat transfer in a horizontal concentric cylindrical annulus using smoothed particle hydrodynamics method (SPH). The governing equations of fluid are discretized into SPH equations and then solved. The modified Rayleigh number was ranging from $10^2$ to $10^7$ and Prandtl number from 0.01 to 10 for the used working fluid. The simulated results are validated with the experimental results and good agreement was obtained. The data revealed that the flow is unstable for the tremendous value of Rayleigh number while it is stable at low value of Rayleigh number. The Rayleigh number in transition region varies with Prandtl number from steady flow to unstable. The results showed also that the Prandtl number affects the flow patterns besides to the transition Rayleigh number.

All previous research has concluded that the increasing of Rayleigh number and the volume of fraction of nanoparticles leads to apparent increasing in the heat transfer rate. Also, the compressive fluid has more significant effect than the non-compressive fluid. The aim of this work is to study and analyze the impact of heat flux, Rayleigh number and ratio (r/R) on the coefficient of natural convective heat transfer with the presence of porous medium, then finding a relation between average Nusselt number with Rayleigh number at different ratio (r/R) and average Nusselt number with (r/R) ratio at different Rayleigh number.

## 2. Mathematical Formulation

The schematic diagram in Figure 1, displays the flow between the inner heated vertical cylinder and the outer cooled cylinder. The outer and inner cylinder are sufficiently long in the axial direction that the end effects can be ignored. In this work, both the inner and outer surfaces of the annular region are assumed to be isothermal. This is equivalent to assuming a high thermal conductivity for both inner and outer surfaces. This isothermal approximation is realistic when the thermal conductivity of both surfaces is at least one order of magnitude higher than that of air [13]. The governing equations of the flow based on the assumptions that: (a) The fluid is 3-D steady, incompressible, and the flow is laminar, (b) no internal heat sources in the fluid and its bounding inner and outer solid walls which have the same thermal conductivity, (c) All fluid properties except air density are taken to be constant and are evaluated at the mean temperature $T_m = (T_i + T_o)/2$, (d) The convective fluid and the porous medium are everywhere in local thermodynamic equilibrium. Two heat fluxes have been supplied 300, 450 W/m$^2$ and various diameter ratio (r/R=0.12,0.20, 0.26) to plot the stream functions and the temperature profiles for the case study. The inner and the outer steel cylinders thickness are (2 mm and 8mm) respectively with equal length of 27cm. The gap between the two cylinders was filled with a porous medium having thermal properties taken from [14].

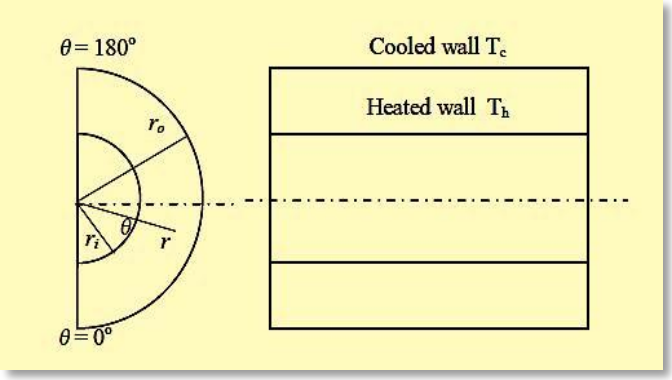


**Fig. 1.** Free convection in porous medium filled annulus

## 3. Governing Equations

The free convection heat transfer governing equations with porous medium in single-phase model consists of continuity, Navier-Stoke's equations which are used for calculating velocity vector and energy equation [15], which is used for calculating the temperature distribution and coefficient of wall heat transfer. It is worth mentioning that the flow in a cylindrical geometry can be described by taking only 2-D because of the axisymmetric nature of the cylinder. For steady, axisymmetric flow, the governing equations in dimensionless form for an incompressible fluid-saturated porous medium which incorporates both the Brinkman and Forschheimer modifications may be expressed as Suhil and Sabty [16].

### *3.1 Fluid Domain*

$$\frac{\partial U_1}{\partial R}+\frac{\partial V_1}{\partial Z}=0 \tag{1}$$

$$U_1\frac{\partial U_1}{\partial R}+V_1\frac{\partial U_1}{\partial Z}=-\frac{\partial P_1}{\partial R}+\Pr\left(\frac{\partial^2 U_1}{\partial R^2}+\frac{\partial^2 U_1}{\partial Z^2}-\frac{U_1}{R^2}\right) \tag{2}$$

$$U_1\frac{\partial V_1}{\partial R}+V_1\frac{\partial V_1}{\partial Z}=-\frac{\partial P_1}{\partial Z}+\Pr\left(\frac{\partial^2 V_1}{\partial R^2}+\frac{\partial^2 V_1}{\partial Z^2}\right)+Ra^*\Pr\theta_1^* \tag{3}$$

$$U_1\frac{\partial \theta_1^*}{\partial R}+V_1\frac{\partial \theta_1^*}{\partial Z}=\left(\frac{\partial^2 \theta_1^*}{\partial R^2}+\frac{\partial^2 \theta_1^*}{\partial Z^2}\right) \tag{4}$$

The dimensionless variables are:

$$U=\frac{uD}{\alpha_f}\ ,\ V=\frac{vD}{\alpha_f}\ ,\ R=\frac{r}{D}\ ,\ Z=\frac{z}{D}\ ,\ P=\frac{pD^2}{\alpha_f\alpha_f^2}\ ,\ D=(r_o-r_i)\ \text{ and }\ \theta^*=\frac{(T-T_o)k_f}{q''D} \tag{5}$$

### *3.2 Porous Domain*

$$\frac{\partial U_2}{\partial R}+\frac{\partial V_2}{\partial Z}=0 \tag{6}$$

$$U_2\frac{\partial U_2}{\partial R}+V_2\frac{\partial U_2}{\partial Z}=-\frac{\partial P_2}{\partial R}+\Pr\left(\frac{\partial^2 U_2}{\partial R^2}+\frac{\partial^2 U_2}{\partial Z^2}-\frac{U_2}{R^2}\right)-\frac{\Pr}{Da}U_2-\Lambda\sqrt{U_2^2+V_2^2}U_2 \tag{7}$$

$$U_2\frac{\partial V_2}{\partial R}+V_2\frac{\partial V_2}{\partial Z}=-\frac{\partial P_2}{\partial Z}+\Pr\left(\frac{\partial^2 V_2}{\partial R^2}+\frac{\partial^2 V_2}{\partial Z^2}\right)+Ra^*\Pr\theta_2^*-\frac{\Pr}{Da}V_2-\Lambda\sqrt{U_2^2+V_2^2}V_2 \tag{8}$$

$$U_2\frac{\partial \theta_2^*}{\partial R}+V_2\frac{\partial \theta_2^*}{\partial Z}=\mathrm{K}\left(\frac{\partial^2 \theta_2^*}{\partial R^2}+\frac{\partial^2 \theta_2^*}{\partial Z^2}\right) \tag{9}$$

where

$$Ra^* = \frac{g\beta q'' D^4}{k_f \alpha_f \upsilon_f} \ , \ Da = \frac{K}{D^2} \ , \ \Lambda = \frac{C_F D}{\sqrt{K}} \quad \text{and} \quad Pr = \frac{\upsilon}{\alpha} \tag{10}$$

The average Nusselt number is defined as

$$\overline{Nu} = \frac{\bar{h} D}{k_f} \tag{11}$$

*3.3 Dimensionless Boundary Conditions*

Wall conditions (no slip conditions at the wall)

$$\begin{aligned} U_1\left(R=\frac{r_o}{D},Z\right)=U_2\left(R=\frac{r_o}{D},Z\right)=V_1\left(R=\frac{r_o}{D},Z\right)=V_2\left(R=\frac{r_o}{D},Z\right)=0 \\ U_1\left(R=\frac{r_i}{D},Z\right)=U_2\left(R=\frac{r_i}{D},Z\right)=V_1\left(R=\frac{r_i}{D},Z\right)=V_2\left(R=\frac{r_i}{D},Z\right)=0 \end{aligned} \tag{12}$$

Inlet and outlet conditions

$$\begin{aligned} P(R,0) = P(R,Z=\frac{L}{D}) \\ \theta_1^*(R,0)=\theta_2^*(R,0)=0 \end{aligned} \tag{13}$$

$$\left.\frac{\partial U_1}{\partial R}\right|_{Z=L/D}=0 \ , \ \left.\frac{\partial U_2}{\partial R}\right|_{Z=L/D}=0 \ , \ \left.\frac{\partial \theta_1^*}{\partial R}\right|_{Z=L/D}=0 \tag{14}$$

Interface boundary conditions (between the porous and clear regions)

$$U_1 = U_2 \ , \ V_1 = V_2 \ , \ P_1 = P_2 \quad \text{and} \quad \frac{\partial \theta_1^*}{\partial R} = k_r \frac{\partial \theta_2^*}{\partial R} \tag{15}$$

$$\frac{\partial U_1}{\partial R} + \frac{\partial V_1}{\partial Z} = \frac{\mu_{eff}}{\mu}\left(\frac{\partial U_2}{\partial R} + \frac{\partial V_2}{\partial Z}\right) \tag{16}$$

Inner and outer cylinder condition (between the porous and clear regions)

$$(fluid\ zone)\ k_r \left.\frac{\partial \theta_1^*}{\partial R}\right|_{R=ri/D} = (porous\ zone)\ k_r \left.\frac{\partial \theta_2^*}{\partial R}\right|_{R=ri/D} = 1 \tag{17}$$

$$(outer\ insulated\ wall)\ \left.\frac{\partial \theta_1^*}{\partial R}\right|_{R=ro/D} = 0 \tag{18}$$

## 4. Numerical Methodology

For modelling heat transfer and flow of fluid in complex engineering geometries, FLUENT v. 15.0 computer program based on finite volume method with hybrid scheme is used. In this program the set of partial differential governing equations (mass, momentum and energy) are solved in three dimensions. An implicit linearization technique is applied in the segregated solution of the modelled equations previously described. This results in a linear system of equations at each computational cell. The equations are coupled and non-linear; therefore, several iterations of the equation set are required to obtain a converged solution. To include the transfer of heat within the solid and fluid for complex model, the FLUENT is the optimal choice for this problem. Due to heat transfer to fluid, the fluid density changes with temperature, as a result the fluid flow can be occurred because of the gravity force which affect the density change. The case study induced with porous medium has been modelled using commercial software, Fluent and software of mesh generation, SOLIDWORKS. SolidWork was employed to build the grid, as shown below in Figure 2. The element type was used to mesh the problem is quadrilateral element. To discretize the momentum equations in three dimensions, SIMPLE algorithm and hybrid-differencing scheme are used to solve the Navier-Stokes and energy equations [17]. Convergence criteria were set to less than $1\times10^{-4}$ for continuity and momentum residuals while set to less than $1\times10^{-8}$ for energy. A final convergence criterion specified in the CFD simulations is based on an overall steady-state energy balance. When the energy imbalance between cylinders is at or below about 2%, the flow simulation is assumed to be at steady state. Therefore, when the residuals are reduced by 4 to 5 orders of magnitude and the energy imbalance is about 2% or less, the flow simulation is complete.

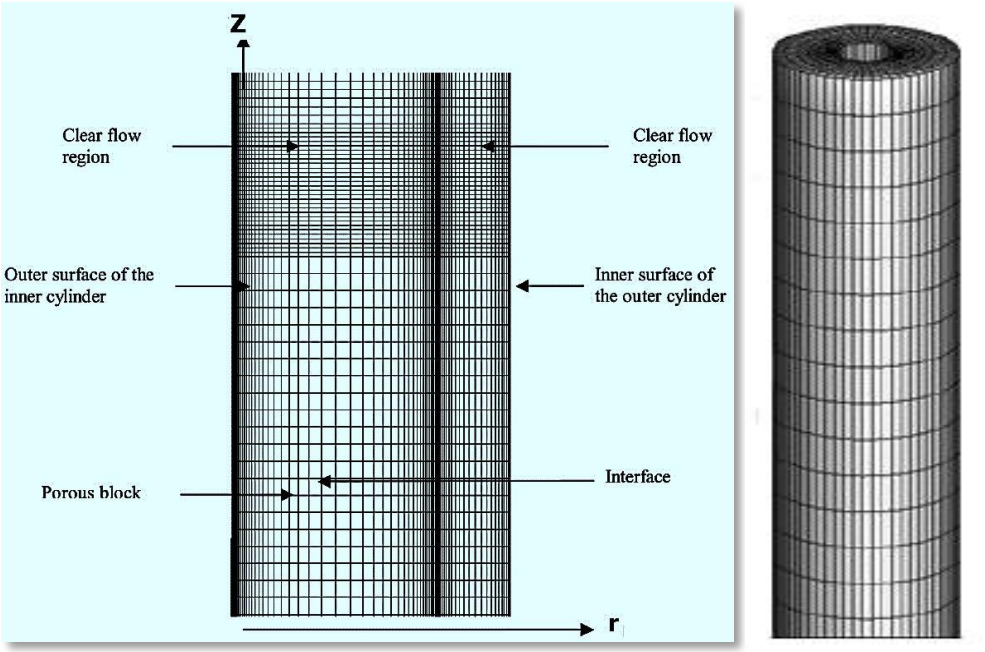


**Fig. 2.** Mesh grid in SolidWorks

### *4.1 Grid Specifications for Concentric Cylinders*

Fifty-one divisions have been included for the radial discretization. Cell clustering was used for the radial divisions at the inner and outer cylinder walls (refer to Figure 3). Factor of cell clustering of 1.2 is applied in the radial direction for each geometry. Cell clustering in the near-wall region is

necessary to resolve changes in the temperature and velocity in the boundary layer due to interactions with the wall. Adding of more cell clustering is based on an order-of-magnitude analysis that provides the order of magnitude for the laminar thermal boundary layer thickness of a plane wall [15].

$$\delta_T \propto \frac{H}{Ra_H^{0.25}} \tag{19}$$

where $H = R\theta$ is defined as the distance along the cylinder wall and $Ra_H$ is a Rayleigh number based on this distance. The increasing and decreasing of $Ra_H$ requiring finer resolution at the walls of cylinder to resolve the thin boundary layer. Same cell clustering factor of 1.2 has been used for each of the concentric cylinders. It is easy to relate the thermal and viscous boundary layer thickness through the working fluid (Pr) number. For (Pr) number fluids of 0.7, the laminar viscous boundary layer is only slightly less than the thermal boundary layer thickness as shown by the expression Bejan [15].

$$\frac{\delta_v}{\delta_T} \sim \mathrm{Pr}^{0.5} \tag{20}$$

where $\delta_v$ is the viscous boundary layer thickness. Therefore, if the clustering of the cell is enough for resolving the thermal boundary layer, it is also enough to determine the viscous boundary layer as long as the local velocity gradients are captured. The solution variables changes decrease away from the thermal and viscous boundary layers. A clustering factor of 1.03 was used from the top to down direction for the angular distribution in the geometry. The computational mesh and cell clustering at the cylinder walls and on the boundaries of symmetry.

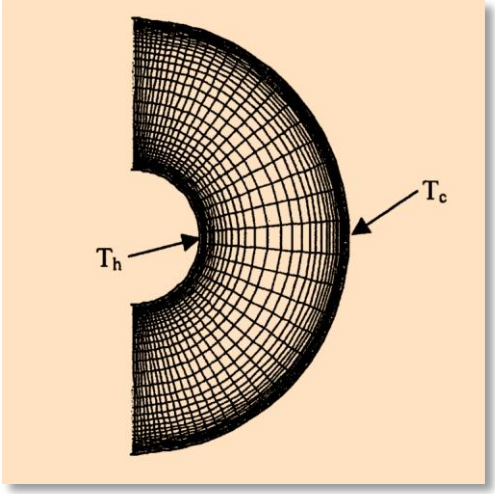


**Fig. 3.** Computational grid for concentric cylinder geometry

*4.2 Stability and Grid Independence Test*

The stability of the numerical simulation is tested for the case Ra=400, (r/R) =0.20, Pr = 0.7. Three-time steps are chosen with values $1\times10^{-4}$, $5\times10^{-4}$, $5\times10^{-6}$. The high difference between the Nusselt

values with various time steps is 2%. The grid-independence is investigated for the same case. Three mesh sizes of (51×61), (81×81), and (91×81) are used for study. The coarse and refined grid contains 3111 (51x61) cells and 6561 (81x81) cells, respectively. Additional refinement contains 7371 cells (91x81) takes place in the angular direction. Table 1 gives the overall heat transfer rates from the inner cylinder to the outer cylinder as a function of the Rayleigh number.

**Table 1**
Grid independence test for heat transfer rates

| Rayleigh number | Coarse grid (51x61) | Refined grid (81x81) | Angular refined grid (91x81) |
|---|---|---|---|
| 400 | 14.1 W | 13.83W | 13.97W |

Some of the differences (a few percent of each other) in the case shown in Table 1 are belong to the inaccurate of using the energy imbalance as the steady state stopping point. Therefore, the CFD results are reasonably independent of the grid. It is also observed that the streamline and isotherm patterns obtained for r/R = 0.26 and Ra = 400 with a 51 x 61 grid and a 81 x 81 grid are in excellent agreement with each other and the maximum difference values in these two grids not exceed 2% for stream function. These contours are not shown because of the space considerations. After these grids' independent tests, a 51x 61 grid is used for all calculations.

## 5. Results and Discussion

### *5.1 Validation Test*

To test the validation of code, the case study for a low temperature outer circular cylinder and high temperature inner circular cylinder was tested. The calculations of simulated average Nusselt numbers are compared with the experimental values taken from Suhil and Sabty [16]. Figure 4 demonstrated the relation between experimental numerical Nu which showed a good agreement between them. Note that the heat transfer behavior experimentally and numerically were the same.

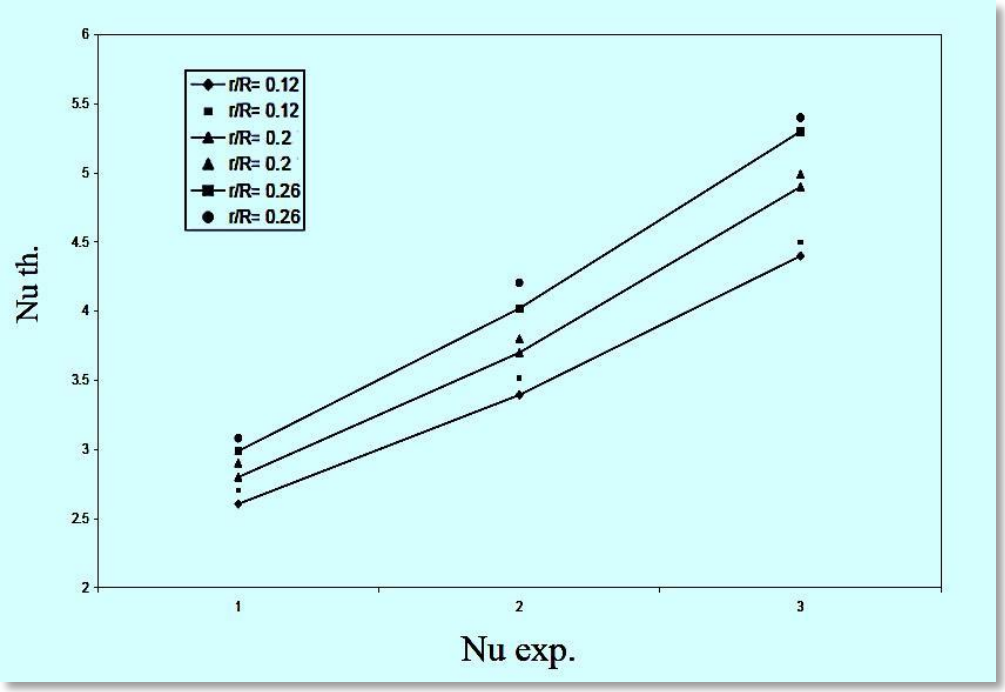


**Fig. 4.** The relation between experimental Nu and numerical Nu

### *5.2 Contour of Temperature*

Figure 5 demonstrated the profiles of temperature at diameter ratio (r/R=0.12), where the red lines represent the profile near the hot side while the blue lines represent the profile of temperature closed cold side, and the maximum temperature value was 171°C for heat flux 300 W/m$^2$. Figure 6 showed the profiles of temperature at diameter ratio (r/R=0.12), which had the same behavior and the high temperature value was 298 °C for heat flux 450 W/m$^2$. Figure 7 displayed the temperature profiles for ratio (r/R=0.20), and the maximum value of temperature was obtained 113°C for heat flux 300 W/m$^2$. Figure 8 exhibited the temperature profiles for ratio (r/R=0.20) which had the same behavior, and the high temperature value was 182 °C for heat flux 450 W/m$^2$. The temperature profiles for ratio (r/R=0.26) and heat flux 300 W/m$^2$ has been presented in Figure 9. The contour showed that the maximum temperature value was 97.8 °C. The same behavior can be clearly observed in the Figure 10, which represent the temperature profiles for ratio (r/R=0.26) and heat flux 450 W/m$^2$ and the highest temperature value obtained was 236 °C. Figure 5 to 10 showed that the increasing of space of gap and value of heat flux leads to rise the hot area for the cold area. Also, for higher Rayleigh numbers, the heat transfer by convection is dominated as noted by the distorted isotherms and low boundary layer thickness. The thermal boundary layer along the inner cylinder separates away from the top point and strikes the outer cylinder around the top region, and then the fluid flows towards the bottom near the outer cylinder. A temperature inversion has been existed in the area between the two thermal boundary layers.

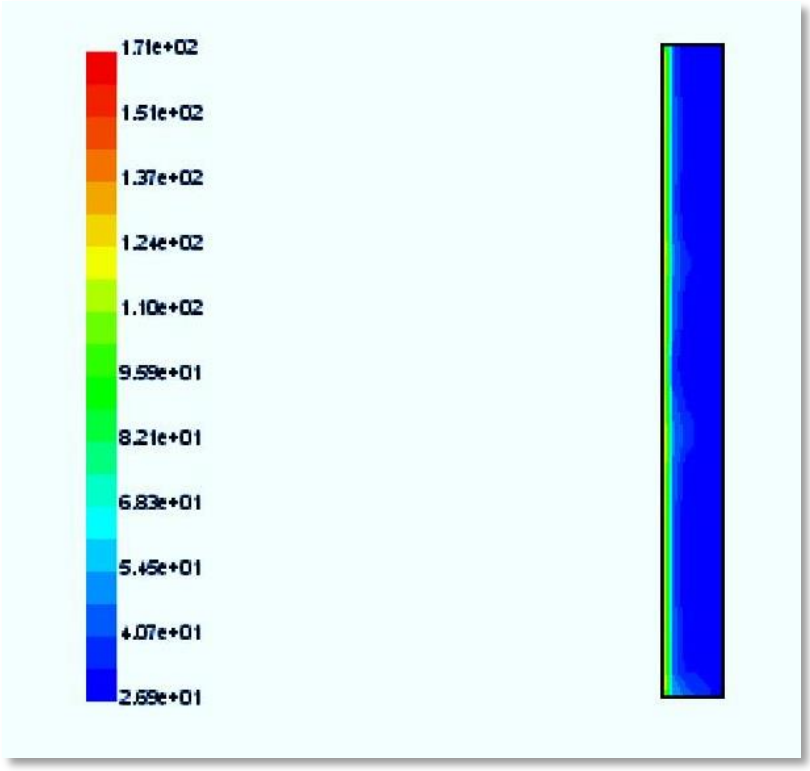


**Fig. 5.** Temperature profiles contour heat flux (300W/m$^2$) and (r/R=0.12)

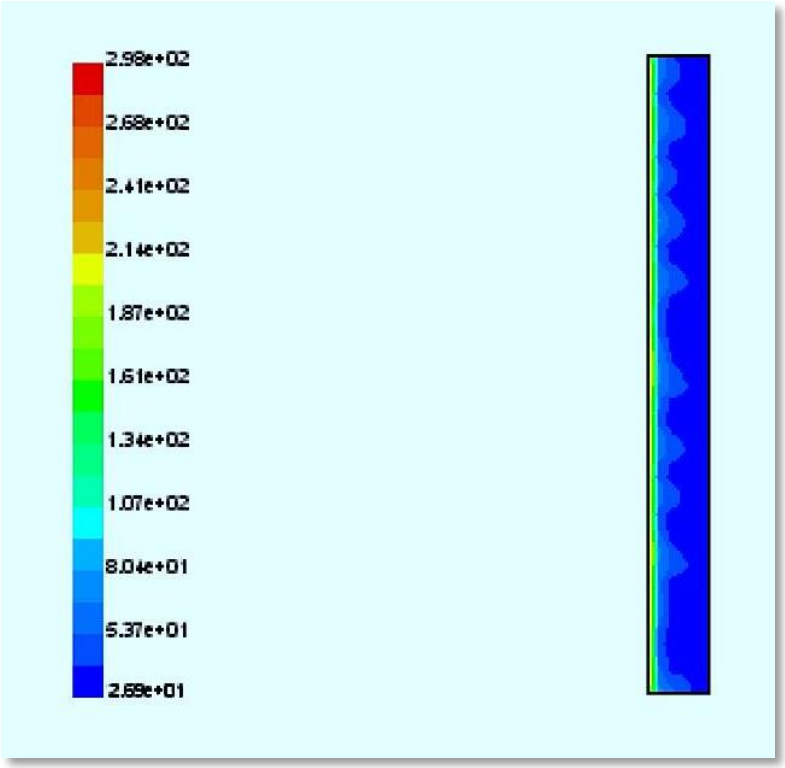


**Fig. 6.** Temperature profiles contour heat flux (450W/m$^2$) and (r/R=0.12)

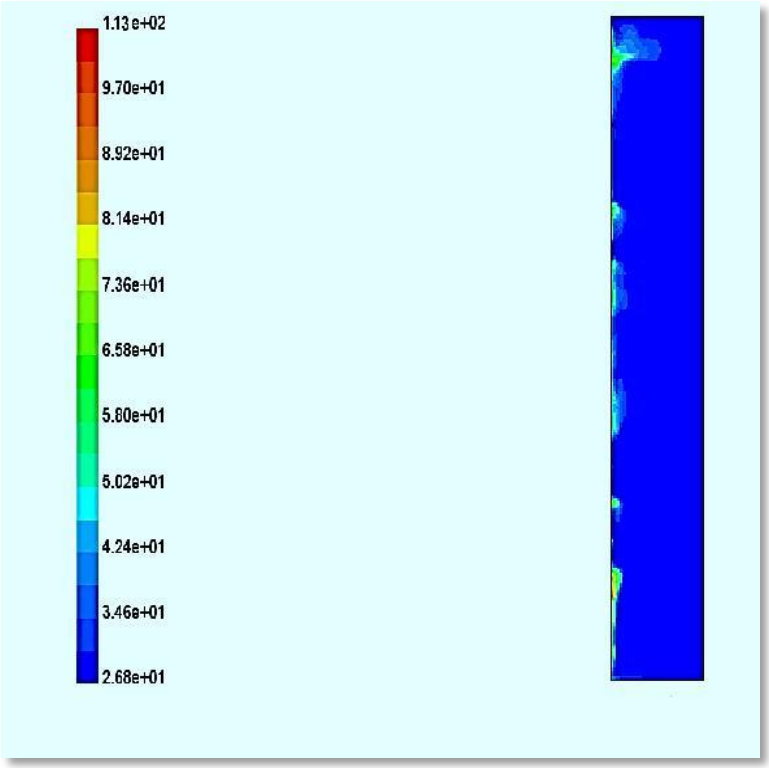


**Fig. 7.** Temperature profiles contour heat flux (300W/m$^2$) and (r/R=0.20)

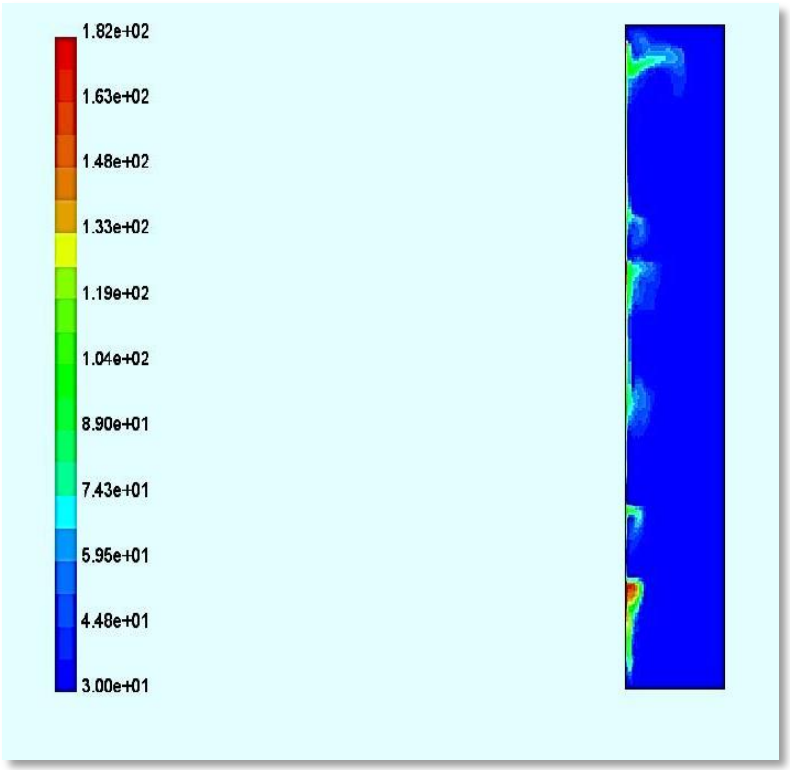


**Fig. 8.** Temperature profiles contour heat flux (450W/m$^2$) and (r/R=0.20)

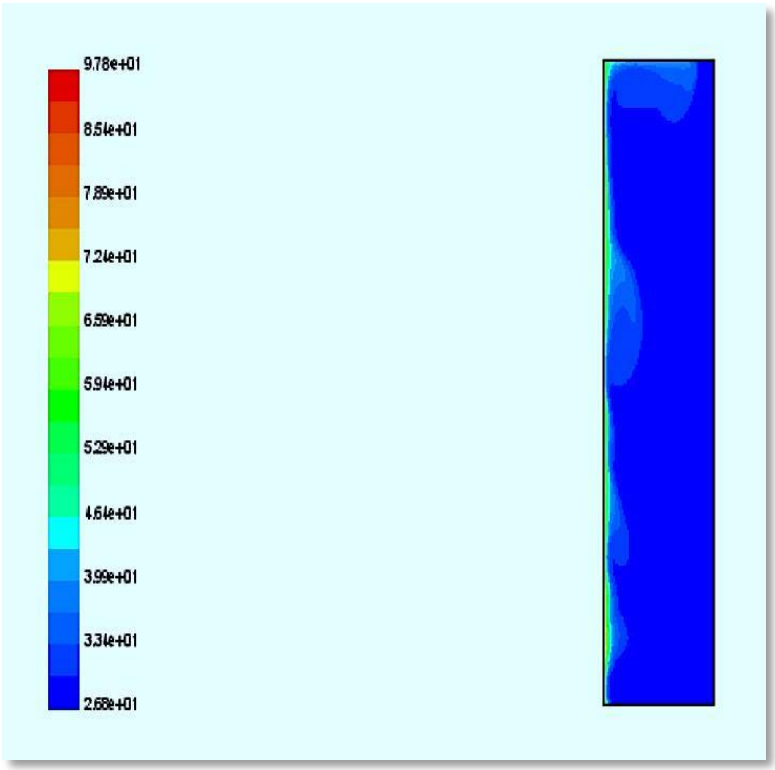


**Fig. 9.** Temperature profiles contour heat flux (300W/m$^2$) and (r/R=0.26)

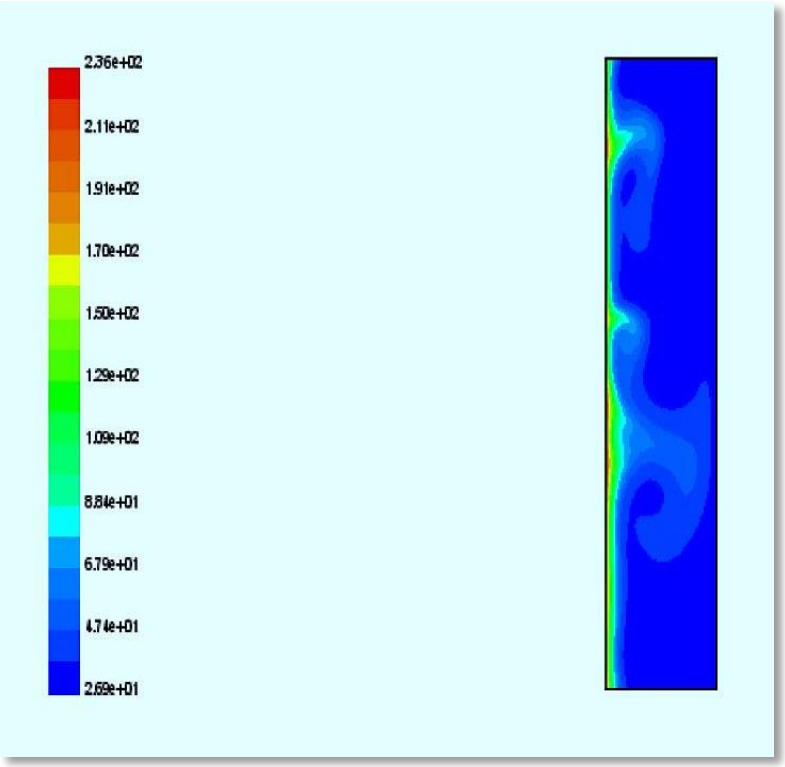


**Fig. 10.** Temperature profiles contour heat flux (450W/m$^2$) and (r/R=0.26)

*5.3 Contour of Stream Function*

Figure 11 displayed the eddy that represent the stream function. The red spot location in the gap centre, while the blue lines are near the wall and the maximum value was 0.884 for heat flux 300W/m$^2$. The stream function for heat flux 450W/m$^2$ and diameter ratio (r/R=0.12) was demonstrated in Figure 12, and the maximum value is (0.046). Figure 13 and 14 showed the stream function for diameter ratio (r/R=0.20) and heat fluxes 300 and 450W/m$^2$, respectively. The highest values were obtained are 1.51 and 0.740, respectively. Figure 15 and 16 indicated the stream function for diameter ratio (r/R=0.26) and heat fluxes 300 and 450W/m$^2$, respectively. The highest values were obtained are 2.5 and 5.13, respectively.

The increasing of stream function value associated with the increasing of gap space and value of heat flux, as shown in Figure 11 to 16. The fluid near the inner cold surface moves downwards while the fluid near the hot surface moves upwards. This recirculation resulting from the merge of two thermal boundary layers, creating cellular configuration. The increasing of Rayleigh number leads to move the cellular configuration location upwards, and when Rayleigh number reaches 450, the flow becomes unsteady which translates to asymmetric and distorted streamlines, as shown in Figure 14. With the increasing of Rayleigh number, the core of circulation is further confined at the top region while forming a secondary core.

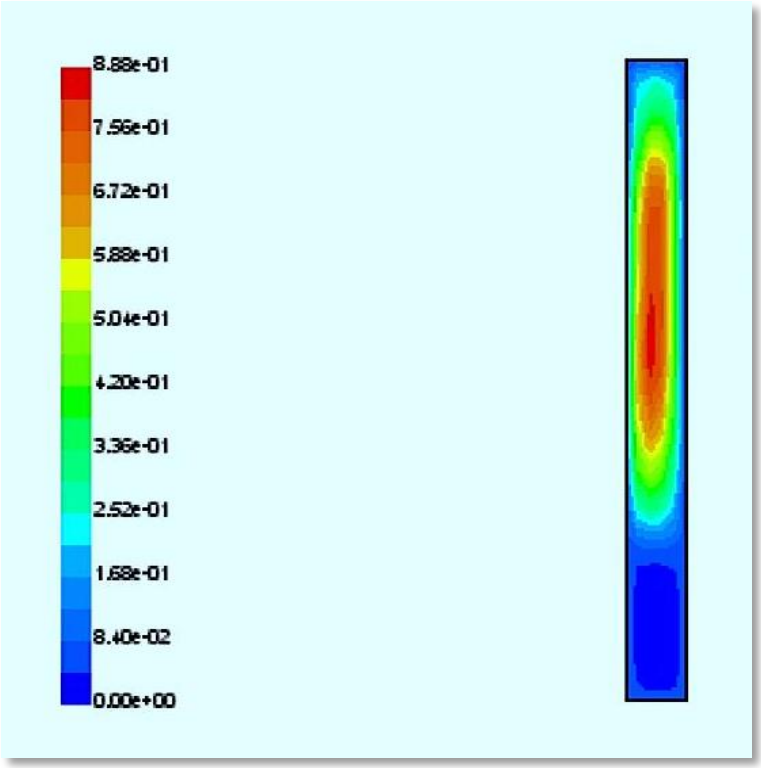


**Fig. 11.** Stream function contour heat flux (300W/m$^2$) and (r/R=0.12)

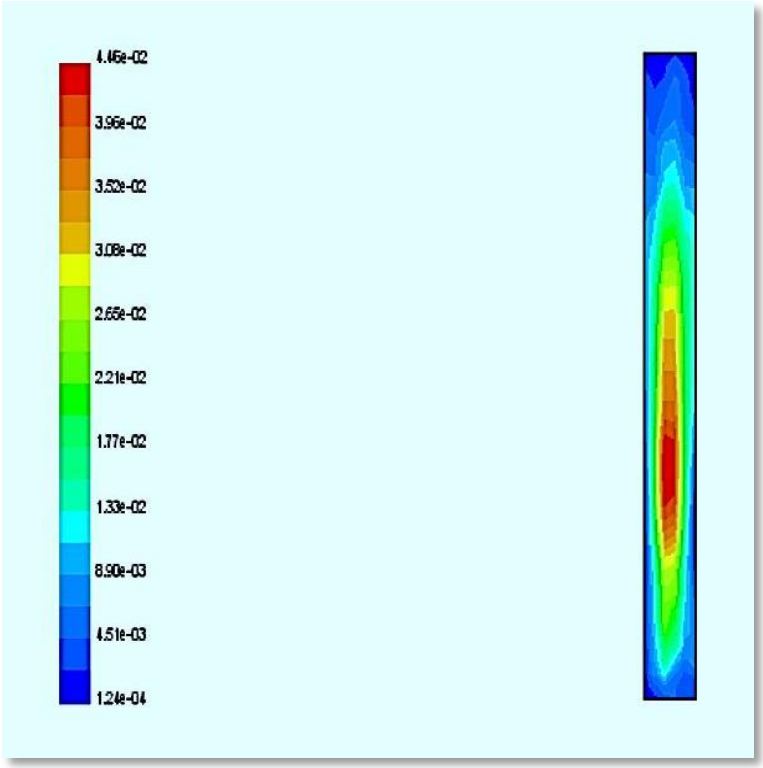


**Fig. 12.** Stream function contour heat flux (450W/m$^2$) and (r/R=0.12)

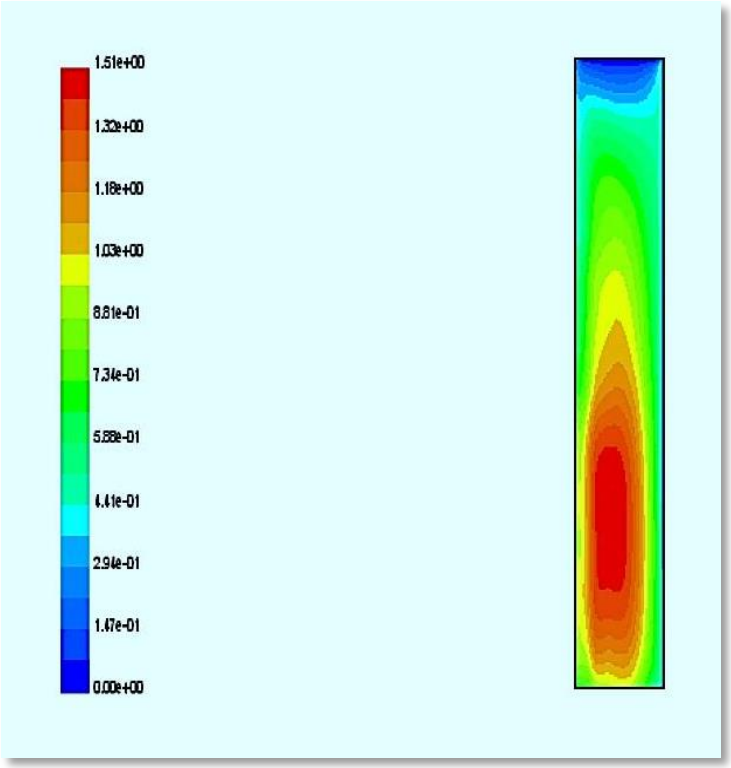


**Fig. 13.** Stream function contour heat flux (300W/m$^2$) and (r/R=0.20)

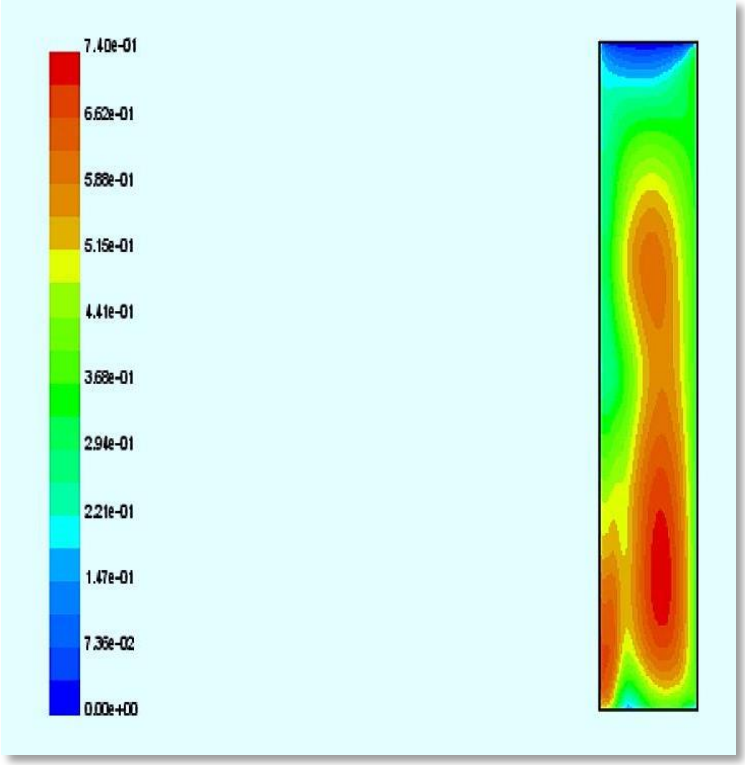


**Fig. 14.** Stream function contour heat flux (450W/m$^2$) and (r/R=0.20)

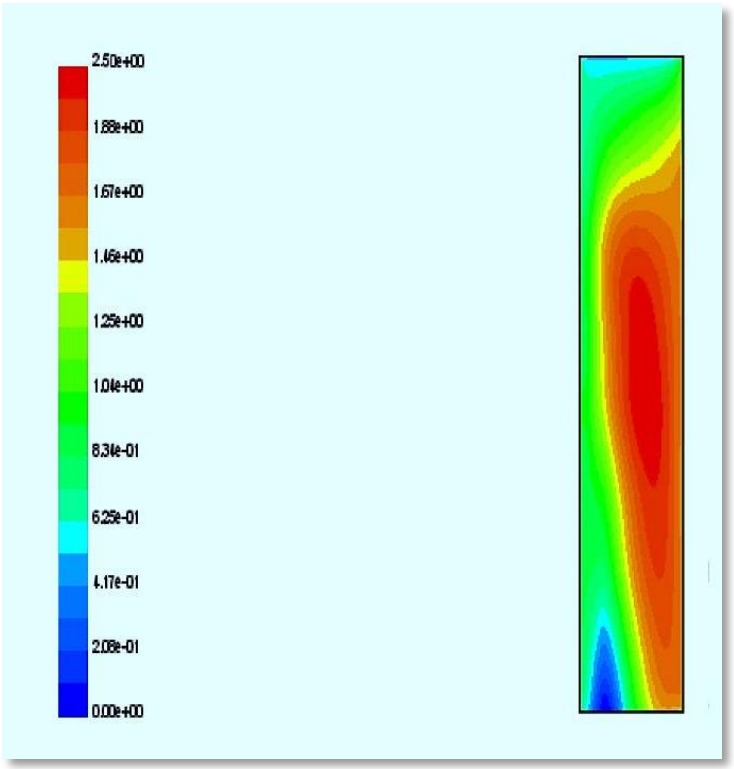


**Fig. 15.** Stream function contour heat flux (300W/m$^2$) and (r/R=0.26)

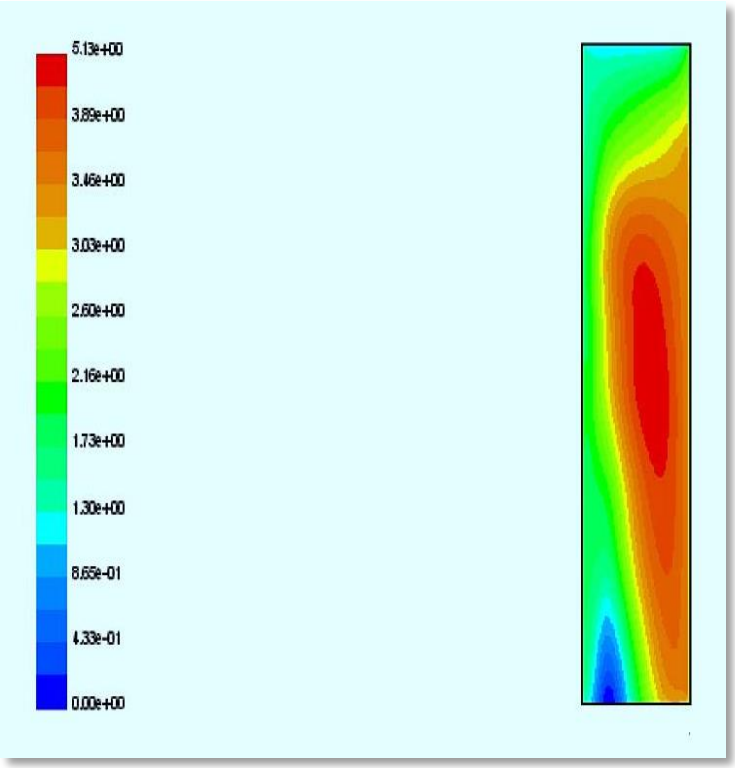


**Fig. 16.** Stream function contour heat flux (450W/m$^2$) and (r/R=0.26)

### *5.4 Heat Transfer Correlations*

Heat transfer in the domain is represented by the average Nusselt number. Depending on many simulations runs, we developed correlations based on Rayleigh number at three pertinent reference radius ratios. Since the total average Nusselt number at the inner cylinder is approximately the same as that at the outer shape entity (<1% difference). The average Nusselt number values at the annulus entrance are very high because of the zero thickness of boundary layer, and the natural convection is very low in this region, then increase gradually downstream because of the natural convection increasing. The changing of average Nusselt number based on three various radius ratios at different heat fluxes is shown in Figure 17. As can be seen, the higher radius ratio resulted in a higher Nusselt number in all cases and the relation between them.

$$Nu = 1.6942\ e^{4.4535(r/R)} \tag{21}$$

Figure 18 showed that the Nusselt number is a function of Rayleigh number at different diameter ratio (r/R). It can be observed that the free convection heat transfer increasing resulting from the heat flux increasing which acting by number of Rayleigh and all the points as can be seen are represented by linearization of the following equation.

$$Nu = 1.5864\ e^{0.0029Ra} \tag{21}$$

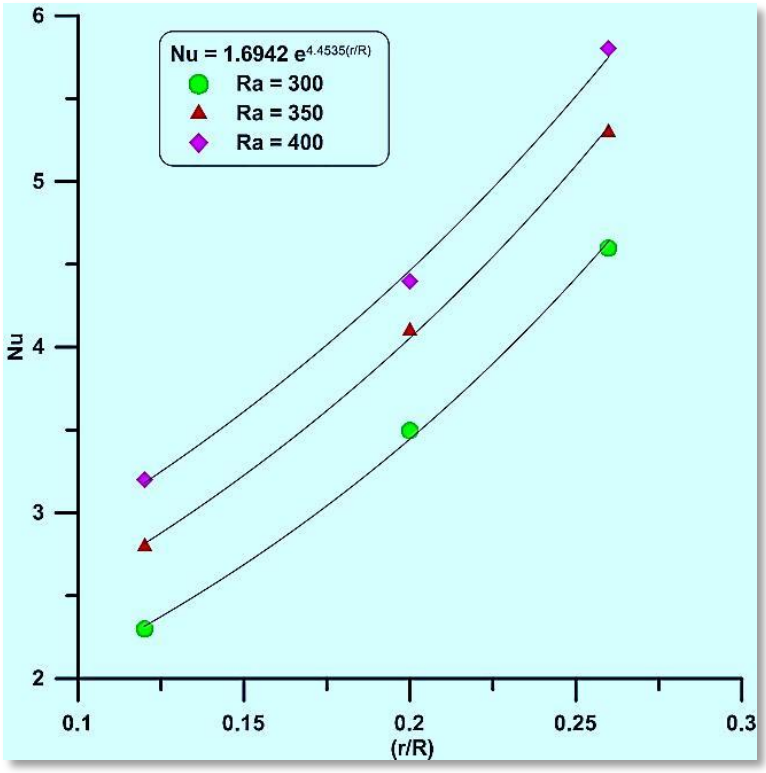


**Fig. 17.** Nusselt number versus ratio (r/R) at various Rayleigh number

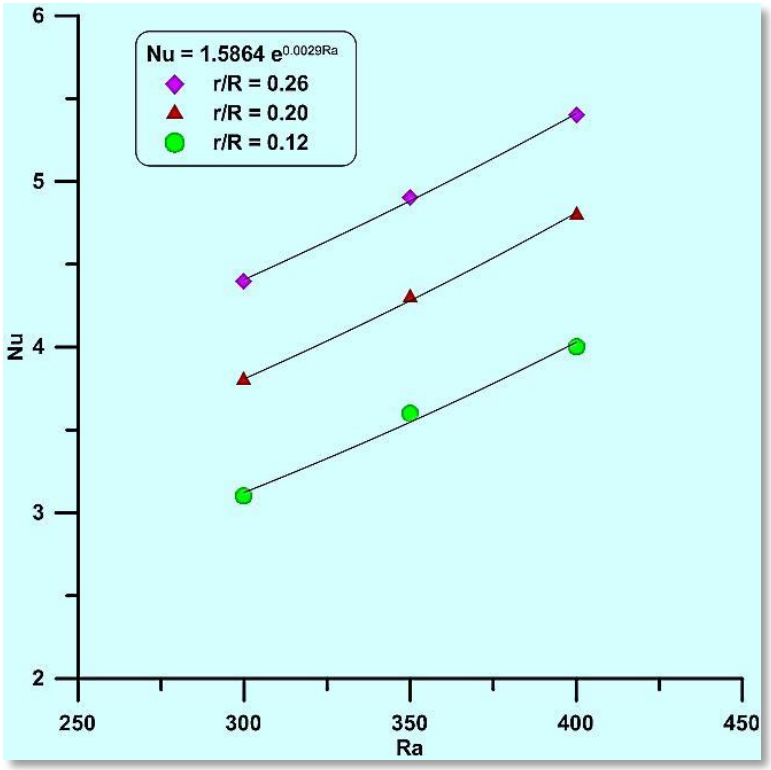


**Fig. 18.** Nusselt number versus Rayleigh number at various ratio (r/R)

## 6. Conclusions

Influence of the presence of the porous media on the free convection heat transfer from circular vertical cylinder in a circular enclosure was investigated numerically over a fairly wide range of (Ra) with taking the effect of annular diameter ratios. A series simulation was conducted in the range of Rayleigh number $300 \leq Ra \leq 400$ and Prandtl number $Pr = 0.7$. In this work the parameters of geometry were modified and the effects of eccentricities of cylinders was not studied, which can be the topic of future work. Quantities obtained numerically include temperature distribution, stream function contours and average Nusselt numbers. The main conclusions of the present work can be summarized as follows.

i. The numerical results show that the Nusselt number increases with increasing the Rayleigh number for all cases.
ii. The average Nusselt number enhances gradually when the diameter ratios are increased from 0.12 to 0.26 for each Rayleigh number.
iii. The comparison of the average Nusselt number obtained from the experimental measurements and the numerical simulations based on the kinetic approach was carried out, and good agreement with available previous published results have been obtained.
iv. The effect of buoyancy is small at the annulus entrance and increase downstream.
v. At different heat fluxes and for any diameter ratio, the profiles of temperature and the stream functions behavior were the same.
vi. The Nusselt number is a function of diameter ratio and the relation between them was $Nu = 1.6942\ e^{4.4535(r/R)}$
vii. The Nusselt number is a function of Rayleigh number and the relation between them was $Nu = 1.5864\ e^{0.0029Ra}$

## Acknowledgement
The authors wish to thank (Dr. Bassim M. Majel) for their continued support of this research.

## References
[1] Kuehn, T. H., and R. J. Goldstein. "An experimental and theoretical study of natural convection in the annulus between horizontal concentric cylinders." *Journal of Fluid mechanics* 74, no. 4 (1976): 695-719.
[2] Projahn, U., and H. Beer. "Prandtl number effects on natural convection heat transfer in concentric and eccentric horizontal cylindrical annuli." *Wärme-und Stoffübertragung* 19, no. 4 (1985): 249-254.
[3] El-Shaarawi, M. A. I., M. A. Al-Nimr, and M. A. Hader. "Transient conjugated heat transfer in concentric annuli." *International Journal of Numerical Methods for Heat & Fluid Flow* 5, no. 5 (1995): 459-473.
[4] El-Shaarawi, Maged AI, and A. A. A. Negm. "Conjugate natural convection heat transfer in an open-ended vertical concentric annulus." *Numerical Heat Transfer: Part A: Applications* 36, no. 6 (1999): 639-655.
[5] Teertstra, P., and M. M. Yovanovich. "Comprehensive review of natural convection in horizontal circular annuli." *ASME-PUBLICATIONS-HTD* 357 (1998): 141-152.
[6] Mohammed, Akeel A. "Natural convection heat transfer in a vertical concentric annulus." *Journal of Engineering* 13, no. 2 (2007): 1417-1427.
[7] Hassan, Ayad K., and Jasim MA Al-lateef. "Numerical simulation of two-dimensional transient natural convection heat transfer from isothermal horizontal cylindrical annuli." *Engineering and Technology Journal* 25, no. 6 (2007): 728-745.
[8] Francis Jr, Nicholas D., Michael T. Itamura, Stephen W. Webb, and Darryl L. James. *CFD calculation of internal natural convection in the annulus between horizontal concentric cylinders*. No. SAND2002-3132. Yucca Mountain Project, Las Vegas, Nevada (US), 2002.
[9] Yamaguchi, Hiroki, Kazuaki Kanazawa, Yu Matsuda, Tomohide Niimi, Alexey Polikarpov, and Irina Graur. "Investigation on heat transfer between two coaxial cylinders for measurement of thermal accommodation coefficient." *Physics of fluids* 24, no. 6 (2012): 062002.
[10] Yuan, Xing, Fatemeh Tavakkoli, and Kambiz Vafai. "Analysis of natural convection in horizontal concentric annuli of varying inner shape." *Numerical Heat Transfer, Part A: Applications* 68, no. 11 (2015): 1155-1174.
[11] Khalili, Ebrahim, Ahmad Saboonchi, and Mohsen Saghafian. "Natural convection of Al2O3 nanofluid between two horizontal cylinders inside a circular enclosure." *Heat Transfer Engineering* 38, no. 2 (2017): 177-189.
[12] Yang, Xiufeng, and Song-Charng Kong. "Numerical study of natural convection in a horizontal concentric annulus using smoothed particle hydrodynamics." *Engineering Analysis with Boundary Elements* 102 (2019): 11-20.
[13] Tsui, Y. T., and B. Tremblay. "On transient natural convection heat transfer in the annulus between concentric, horizontal cylinders with isothermal surfaces." *International journal of heat and mass transfer* 27, no. 1 (1984): 103-111.
[14] AL-Kamil.M.T. "A Packed Bed Solar Collector In Thermo-siphon Water Heating System." *Journal of Solar Energy Research* 7 (1989): 17.
[15] Bejan, Adrian. *Convection heat transfer*. John wiley & sons, 2013.
[16] Kiwan, Suhil, and Mohammed Sabty Alzahrany. "Effect of using porous inserts on natural convection heat transfer between two concentric vertical cylinders." *Numerical Heat Transfer, Part A: Applications* 53, no. 8 (2007): 870-889.
[17] Adnan M. Hussein, Tahseen A. Tahseen, and Attala H. Jasim. "Free Convection Heat Transfer in Concentric Annulus Vertical Cylinders Filling with Porous Media." *Journal of Tikrit University –Scientific Studies* 3, no.1 (2008): 65-81.